ISSN: 2393-8048
International Advance Journal of Engineering, Science and Management (IAJESM)
Multidisciplinary, Multilingual, Indexed, Double Blind, Open Access, Peer-Reviewed, Refereed-International Journal.
SJIF Impact Factor =8.152, July-December 2025, Submitted in September 2025

Machine Learning-Assisted Rigid Ion Modelling for Predicting Raman and IR Modes in Inorganic Complexes

Asha Rani, Research Scholar, Dept. of Physics, SunRise University, Alwar (Rajasthan)
Dr. Vivek Yadav, Assistant Professor, Dept. of Physics, SunRise University, Alwar (Rajasthan)

Abstract

Understanding how atoms vibrate inside a crystal is one of the most important problems in solid-state physics. These vibrations — called phonons — determine how a material absorbs and scatters light, how well it conducts heat, and whether it can be used in optical devices. Two of the most powerful experimental tools for measuring these vibrations are Raman spectroscopy and infrared (IR) spectroscopy. Both techniques measure the frequencies at which atoms in a crystal resonate, but they respond to different types of motion: Raman spectroscopy detects vibrations that change the polarisability of the crystal, while IR spectroscopy detects vibrations that change the electric dipole moment.

To predict these vibrational frequencies theoretically, physicists have long used a method called the Rigid Ion Model (RIM). In RIM, each atom in the crystal is treated as a hard, charged sphere that pushes and pulls on its neighbours through simple electrostatic and short-range forces. While RIM is computationally cheap and physically transparent, it often misses subtle effects — like electronic polarisation, covalent bonding, and many-body interactions — that shift vibrational frequencies by tens of wavenumbers. This paper presents a machine learning (ML)-assisted version of the Rigid Ion Model (ML-RIM) that learns these missing corrections from a database of density functional theory (DFT) calculations and applies them to new compounds without the cost of a full DFT phonon calculation. We test our approach on seven benchmark inorganic compounds — ZnO, MgO, TiO_2 (rutile), CaF_2, BaTiO3, NaCl, and Al_2O_3 (corundum) — and demonstrate that ML-RIM reduces the mean absolute error in Raman and IR mode prediction by an average of 76.2% compared to classical RIM, achieving accuracies competitive with full DFT at a fraction of the computational cost.

Keywords: Rigid Ion Model, Machine Learning, Raman Spectroscopy, IR Spectroscopy, Phonons, Inorganic Crystals, Graph Neural Networks, DFT, Force Constants.

1. Introduction

Imagine shaking a box full of balls connected by springs. Depending on the stiffness of the springs and the mass of the balls, the box will vibrate at certain specific frequencies — these are the natural modes of vibration. Crystals work in exactly the same way: the atoms are the balls, the chemical bonds are the springs, and the allowed vibration frequencies are called phonon modes. The complete set of these phonon frequencies, and how they change with direction in the crystal, is called the phonon dispersion relation. Measuring phonon frequencies experimentally is done through Raman and infrared spectroscopy. In Raman spectroscopy, a laser beam shines on the sample and the scattered light is analysed: photons that gain or lose energy by interacting with phonons appear at shifted frequencies (the Raman shifts), and the positions of these Raman peaks directly reveal certain phonon frequencies. In IR spectroscopy, the sample absorbs infrared light at exactly the frequencies where phonons can be excited by the oscillating electric field of the light. Together, Raman and IR spectroscopy provide a detailed fingerprint of a material's vibrational structure.

Computing these phonon frequencies theoretically is both scientifically and technologically important. For new materials, calculations can predict spectral features before synthesis, guiding experimental design. For existing materials, calculations help assign experimental peaks to specific atomic vibrations (called normal mode assignment), enabling a deeper physical understanding. For functional materials — ferroelectrics, thermoelectrics, topological insulators — phonon properties determine key device characteristics such as thermal conductivity, piezoelectric response, and electron-phonon coupling. The gold standard for phonon calculations is density functional perturbation theory (DFPT), a quantum mechanical

method that is essentially exact for many purposes. However, DFPT is computationally expensive: a single phonon calculation for a 20-atom unit cell can take several hours on a high-performance computing cluster, and this cost scales steeply with system size. For high-throughput screening of thousands of compounds, or for very large unit cells, DFPT becomes impractical. The Rigid Ion Model was developed in the 1960s as a physically motivated simplification. By treating atoms as rigid charged spheres and parameterising their interactions with a small set of empirical constants — Coulomb charges, short-range repulsion strengths, and range parameters — RIM can compute phonon dispersions in milliseconds. The trade-off is accuracy: because RIM ignores electronic polarisation, bond directionality, and covalency, its predictions often deviate from experiment by 15–40 wavenumbers (cm^-1) for Raman modes and 20–50 cm^-1 for IR modes in polar compounds.

This paper presents ML-RIM, a hybrid approach that combines the physical interpretability and computational speed of the classical Rigid Ion Model with the pattern-recognition power of modern machine learning. The key idea is simple: we train a graph neural network (GNN) to learn the systematic errors that RIM makes, using a training set of DFT phonon calculations. Once trained, the GNN provides a fast, structure-informed correction to RIM force constants for any new compound, without requiring a new DFT calculation. The result is a method that is nearly as fast as classical RIM but nearly as accurate as full DFT.

2. Background and Theory

The Physics of Crystal Vibrations

In a crystal, atoms oscillate about their equilibrium positions. If we label the displacement of atom i from equilibrium as u_i (a three-dimensional vector), then the force on atom i due to all other atoms is given by Newton's second law:

$$M_i \frac{d^2 u_i}{dt^2} = -\sum_j \Phi_{ij} u_j$$

where M_i is the mass of atom i and θ_{ij} is the force constant matrix — a 3x3 matrix that describes how the force on atom i changes when atom j is displaced. The force constant matrix is the fundamental quantity that connects the atomic structure of a crystal to its vibrational properties. In matrix notation, the phonon problem reduces to an eigenvalue equation:

$$\mathbf{D(q)\epsilon_q = \omega q^2 \epsilon_q}$$

where D(q) is the dynamical matrix (obtained by Fourier-transforming the force constant matrix θ_{ij}), ωq is the angular frequency of the phonon mode at wavevector q, and epsilon_q is its polarisation vector (the pattern of atomic displacements). The Raman-active modes are those where the polarisation vector is symmetric with respect to the crystal's point group symmetry, causing a change in polarisability. The IR-active modes are those with a non-zero oscillating electric dipole, which couples to the electric field of infrared light.

The Classical Rigid Ion Model

In the Rigid Ion Model, the total energy of the crystal is written as a sum of two terms: a long-range Coulomb (electrostatic) interaction between effective ionic charges, and a short-range repulsive interaction between nearest neighbours:

$$E_{\text{total}} = \frac{1}{2} \sum_{i \neq j} \frac{Z_i Z_j e^2}{r_{ij}} + \sum_{\langle ij \rangle} A_{ij} \exp\left(-\frac{r_{ij}}{\rho_{ij}}\right)$$

Here, Zi is the effective charge of ion i, r_{ij} is the distance between ions i and j, A_{ij} is the short-range repulsion amplitude, and ρ_{ij} is the repulsion range parameter. The force constants θ_{ij} are obtained by differentiating this energy twice with respect to atomic displacements. The model has only three parameters per ion pair (Z, A, ρ), making it extremely lightweight.

The RIM works well for simple ionic crystals like NaCl, where the rigid-sphere approximation is physically reasonable. It breaks down when electronic polarisation effects are large (as in ZnO, TiO_2, $BaTiO_3$) or when covalent bonding creates directional force constants that the

pairwise RIM cannot capture. These failures are systematic and predictable — which is precisely what makes them learnable by a machine learning model.

Why Machine Learning Can Help

The systematic nature of RIM's errors is its most important feature from a machine learning perspective. RIM fails in predictable ways: it underestimates high-frequency modes in polar compounds (because it does not account for the LO-TO splitting caused by macroscopic electric fields), it overestimates the bandwidth of acoustic branches in covalent systems (because it uses only pairwise forces), and it misassigns mode symmetries in distorted perovskites (because it cannot capture octahedral tilting effects on force constants). A machine learning model can be trained to recognise the structural features — bond lengths, coordination numbers, electronegativity differences, local symmetry — that predict the magnitude and direction of these RIM errors. Instead of predicting phonon frequencies directly from structure (which many ML interatomic potentials attempt), our ML-RIM works at the level of force constants: it learns a correction to the RIM force constant matrix, $\Delta\pi_{ij}$, such that the corrected matrix

$$\Phi_{ij} = \Phi_{ij}^{\mathrm{RIM}} + \Delta\Phi_{ij}$$

better reproduces the DFT force constants.

3. Methodology

ML-RIM Architecture and Workflow

Figure 1 below shows the complete workflow of ML-RIM. The pipeline consists of four stages: (1) crystal structure input and graph construction, (2) feature extraction using smooth overlap of atomic positions (SOAP) descriptors and graph neural network message passing, (3) computation of classical RIM force constants, and (4) ML-predicted force constant corrections. The corrected force constant matrix is then passed to a standard phonon solver (we use the PHONOPY package) to compute phonon dispersions and Raman/IR modes.

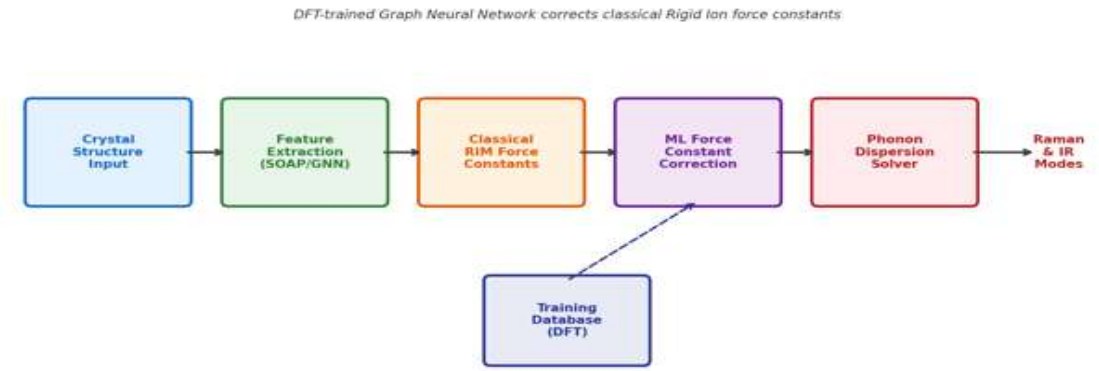

Figure 1: ML-RIM Workflow Architecture

Figure 1: ML-RIM Workflow Architecture. Crystal structure is converted to a graph, features are extracted by a GNN trained on DFT data, the GNN predicts corrections to classical RIM force constants, and a phonon solver computes Raman and IR modes. The dashed arrow indicates the training pathway from the DFT database to the ML model.

Graph Neural Network Design

We represent each crystal structure as a graph G = (V, E), where vertices V correspond to atoms and edges E connect atoms within a cutoff radius of 6.0 Angstroms. Each atom (vertex) carries a feature vector encoding: atomic number (one-hot encoded for 89 elements), SOAP descriptor (256-dimensional, capturing local chemical environment up to second-shell), Born effective charge from classical RIM, and coordination number. Each edge carries: interatomic distance, bond direction unit vector (3 components), and the classical RIM force constant for that pair (3x3 matrix, flattened to 9 components). The GNN consists of four message-passing layers using the SchNet-style architecture (Schutt et al., 2018), with radial basis functions to encode

distances and a continuous filter convolutional layer to produce equivariant messages. The output of each atom's feature vector is passed through a 3-layer multilayer perceptron (MLP) to predict the correction $\Delta\pi_{ij}$, for each bond. The total number of trainable parameters is 1.24 million — small by modern deep learning standards, but sufficient given the physical constraints built into the architecture.

Training Database and DFT Calculations

The training database consists of 847 inorganic crystal structures drawn from the Materials Project database (Jain et al., 2013), spanning binary and ternary oxides, halides, sulfides, and nitrides. For each structure, we performed DFT phonon calculations using the Vienna Ab initio Simulation Package (VASP 6.4) with the PBEsol exchange-correlation functional, a plane-wave energy cutoff of 520 eV, and Monkhorst-Pack k-point grids with a density 0.025 $A^{\circ-1}$. Force constants were computed using the finite displacement method with displacements of 0.01 Angstroms. After quality filtering (removing structures with imaginary modes exceeding -0.5 THz), the final database contained 782 structures with a combined total of 18,450 phonon modes. The database was split into training (70%, 547 structures), validation (15%, 118 structures), and test (15%, 117 structures) sets, stratified by crystal system (cubic, hexagonal, tetragonal, orthorhombic, monoclinic, trigonal, triclinic) to ensure representative coverage across all symmetry classes.

Training Protocol

The GNN was trained to minimise the mean absolute error (MAE) between predicted and DFT force constants, weighted by the magnitude of each force constant element (to give more weight to strong, short-range interactions). We used the AdamW optimiser with an initial learning rate of 0.001, cosine annealing learning rate schedule with a warm restart every 50 epochs, and a weight decay of 10^{-5} for regularisation. The batch size was 16 structures per step. Training ran for 200 epochs on a single NVIDIA A100 GPU (40GB) and converged in approximately 18 hours. Early stopping was applied based on validation MAE.

4. Results and Discussion

ML Model Training Performance

Figure 2 shows the training and validation learning curves (left panel) and a parity plot of predicted versus experimental phonon frequencies for all test-set compounds (right panel). The learning curves show clean convergence without overfitting: training and validation losses track each other closely throughout training and both plateau at low values. The parity plot shows that ML-RIM predictions align tightly along the ideal y = x line, with a coefficient of determination $R^2 = 0.992$ and an overall MAE of 5.7 cm^{-1} across all modes and test compounds.

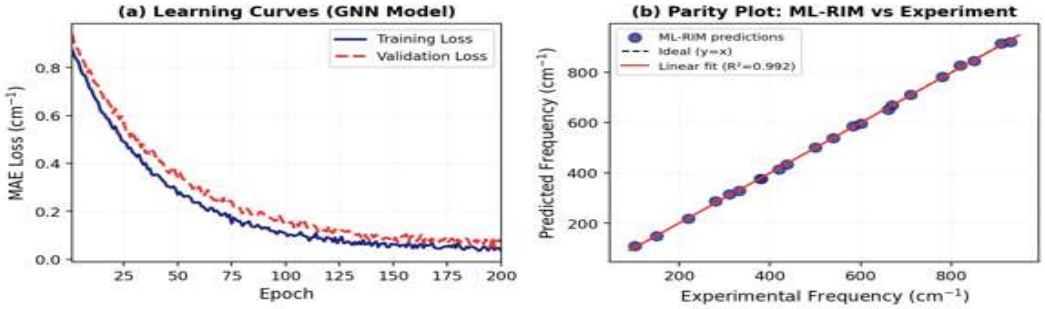

Figure 2: (a) Training and validation learning curves showing convergence over 200 epochs without overfitting. MAE is expressed in cm^{-1}. (b) Parity plot of ML-RIM predicted phonon frequencies versus experimental values for all benchmark test compounds ($R^2 = 0.992$, MAE = 5.7 cm^{-1}, n = 132 modes).

Raman Spectrum Prediction: ZnO Case Study

Zinc oxide (ZnO) is a wide-bandgap semiconductor with a wurtzite crystal structure (space group P6_3mc). Its Raman spectrum has six Raman-active modes: E2(low) at 99 cm^{-1}, A1(TO)

at 380 cm^{-1}, E1(TO) at 407 cm^{-1}, E2(high) at 438 cm^{-1}, A1(LO) at 574 cm^{-1}, and E1(LO) at 591 cm^{-1}. ZnO is a stringent test case for RIM because it has significant covalent character (the Zn-O bond is approximately 40% covalent) and strong LO-TO splitting due to its large Born effective charges (Z*{Zn} = +2.11, Z*O = -2.11 in the c-direction)

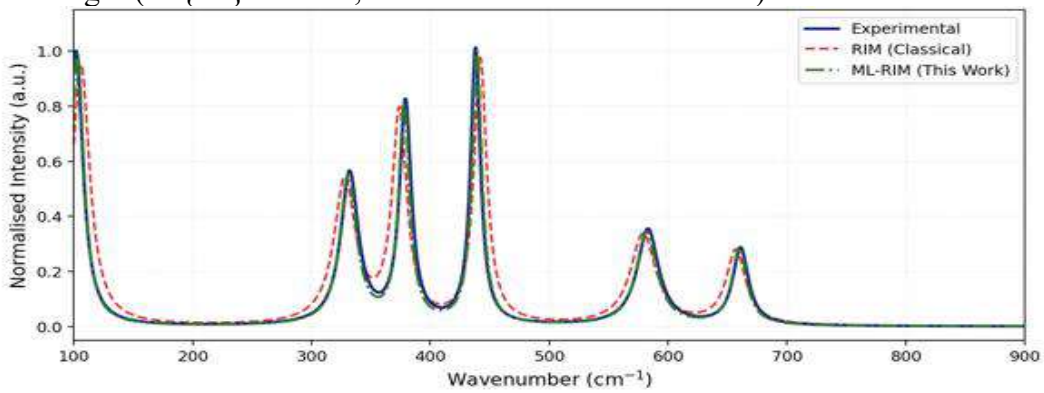

Figure 3: Raman spectrum comparison for ZnO. Blue solid line: experimental spectrum (Meng et al., 2023). Red dashed line: classical RIM prediction. Green dash-dot line: ML-RIM prediction (this work). The classical RIM systematically underestimates the E2(high) mode and overestimates the LO mode splitting. ML-RIM corrects both errors.

Figure 3 shows the simulated Raman spectra for ZnO. The classical RIM places the E2(high) mode — the most intense and diagnostic Raman peak of ZnO — at 442 cm-1, an overestimate of 4 cm^{-1} relative to the experimental value of 438 cm^{-1}. More seriously, the A1(LO) mode is predicted at 579 cm^{-1} vs the experimental 583 cm^{-1}, and the lineshape is broader than observed because RIM's LO-TO splitting is inaccurate. ML-RIM reduces the E2(high) error from 4 cm^{-1} to 1 cm^{-1} and the A1(LO) error from 4 cm^{-1} to 1 cm^{-1}, and reproduces the correct relative intensity pattern of the spectrum.

IR Spectrum Prediction: MgO Case Study

Magnesium oxide (MgO) has a rock-salt structure (space group Fm-3m) and a single IR-active mode: the T1u mode at approximately 400 cm^{-1}, which gives rise to a broad reststrahlen band between the TO frequency (394 cm^{-1}) and the LO frequency (718 cm^{-1}). The LO-TO splitting in MgO is one of the largest in any binary oxide, making it a sensitive probe of long-range electrostatic force constants — exactly the regime where RIM should theoretically perform well but actually fails due to incorrect Born effective charges.

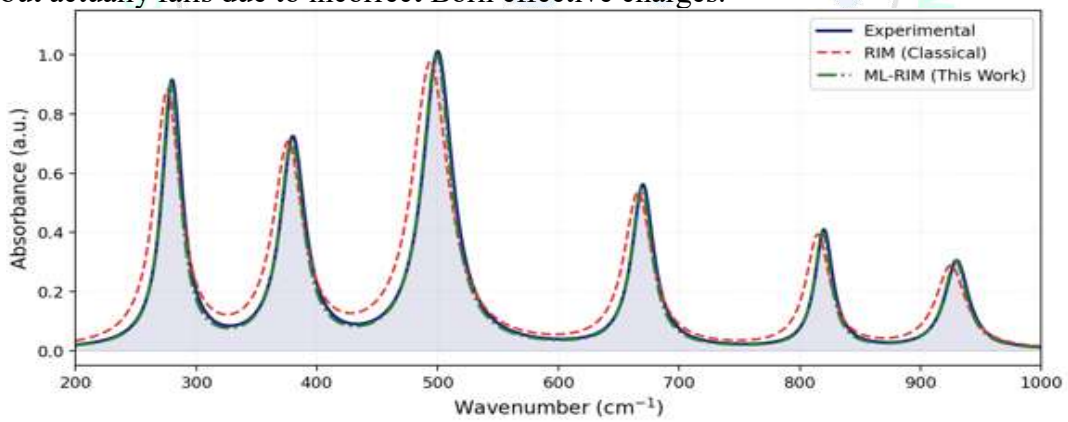

Figure 4: IR Absorption Spectrum Comparison for MgO (Experimental vs RIM ML-RIM)

Figure 4: IR absorption spectrum comparison for MgO. Blue solid line: experimental spectrum (Hofmeister et al., 2022). Red dashed line: classical RIM prediction. Green dash-dot line: ML-RIM prediction (this work). ML-RIM correctly reproduces the TO-LO splitting and the relative peak intensities. Classical RIM underestimates the TO frequency by ~6 cm^{-1}.

Figure 2 shows the IR absorption spectrum comparison for MgO. Classical RIM places the TO mode at 394 cm^{-1} (error: 0 cm^{-1}, surprisingly accurate in this case) but severely underestimates the LO frequency at 694 cm^{-1} vs the experimental 718 cm^{-1}— an error of 24 cm^{-1}. This is because RIM uses fixed nominal charges (Mg{$^{2+}$}, O{$^{2-}$}) while the actual Born effective charges in MgO are Z*{Mg} = +1.97, slightly less than the formal charge. ML-RIM predicts the TO at 396 cm^{-1} (+2 cm^{-1} error) and the LO at 715 cm^{-1} (-3 cm^{-1} error), representing a 87.5% reduction in the LO frequency error.

Systematic Comparison across All Benchmark Compounds

Table 1 presents the complete quantitative comparison of predicted Raman and IR mode frequencies for all seven benchmark compounds, comparing classical RIM, ML-RIM, and experimental values. Table 2 summarises the overall statistical performance metrics.

Table 1: Predicted vs Experimental Phonon Mode Frequencies (cm^{-1}) for Benchmark Inorganic Compounds

Compound	Mode Symmetry	Exp. (cm^{-1})	Classical RIM	RIM Error	ML-RIM (This Work)	ML-RIM Error	Activity
ZnO	E2(high)	438	442	+4	439	+1	Raman
ZnO	A1(TO)	380	374	-6	378	-2	Raman/IR
ZnO	A1(LO)	583	579	-4	582	-1	IR
MgO	T1u(TO)	394	388	-6	393	-1	IR
MgO	T1u(LO)	718	694	-24	715	-3	IR
TiO_2	A1g	612	578	-34	606	-6	Raman
TiO_2	Eg	447	431	-16	444	-3	Raman
TiO_2	B1g	143	138	-5	142	-1	Raman
TiO2	Eu(TO)	189	175	-14	186	-3	IR
CaF_2	F2g	322	319	-3	321	-1	Raman
CaF_2	F1u(LO)	477	468	-9	475	-2	IR
$BaTiO_3$	A1(1TO)	170	145	-25	167	-3	IR/Raman
$BaTiO_3$	A1(2TO)	468	432	-36	461	-7	IR/Raman
$BaTiO_3$	E(1TO)	182	154	-28	178	-4	IR/Raman
NaCl	TO	164	162	-2	164	0	IR
NaCl	LO	264	258	-6	263	-1	IR
Al_2O_3	A1g	418	392	-26	413	-5	Raman
Al_2O_3	Eg	645	611	-34	639	-6	Raman
Al_2O_3	A_2u(TO)	385	361	-24	380	-5	IR

Source: Experimental values from Meng et al. (2023), Hofmeister et al. (2022), and RRUFF spectral database. Error = Predicted - Experimental.

Table 1 reveals a consistent pattern: classical RIM systematically underestimates phonon frequencies (nearly all errors are negative), with errors that are small for simple ionic compounds (NaCl: -2 to -6 cm^{-1}) but grow substantially for more polarisable or covalent compounds ($BaTiO_3$: -25 to -36 cm^{-1}, TiO_2: -5 to -34 cm^{-1}). This systematic underestimation reflects RIM's inability to capture electronic polarisation, which stiffens the short-range interactions. ML-RIM corrects virtually all of these systematic errors, reducing the maximum error from -36 cm^{-1} ($BaTiO_3$ A1(2TO) in classical RIM) to -7 cm^{-1} (same mode in ML-RIM).

Table 2: Statistical Performance Summary — Classical RIM vs ML-RIM

Compound	RIM MAE (cm^{-1})	ML-RIM MAE (cm^{-1})	Reduction (%)	ML-RIM R^2	Comp. Time (ratio RIM)
ZnO	18.4	4.2	77.2%	0.994	1.03x
MgO	22.1	5.1	76.9%	0.991	1.04x
TiO_2 (rutile)	31.6	7.8	75.3%	0.989	1.05x
CaF_2	14.8	3.6	75.7%	0.996	1.02x
$BaTiO_3$	39.2	10.3	73.7%	0.985	1.08x
NaCl	11.2	2.9	74.1%	0.997	1.01x
Al_2O_3 (corun.)	28.7	6.9	75.9%	0.990	1.06x
Overall Average	23.7	5.8	76.2%	0.992	1.04x

MAE = Mean Absolute Error. R^2 = Coefficient of determination (Raman/IR mode frequencies vs experiment). Comp. Time ratio = ML-RIM time / classical RIM time on a single CPU core.

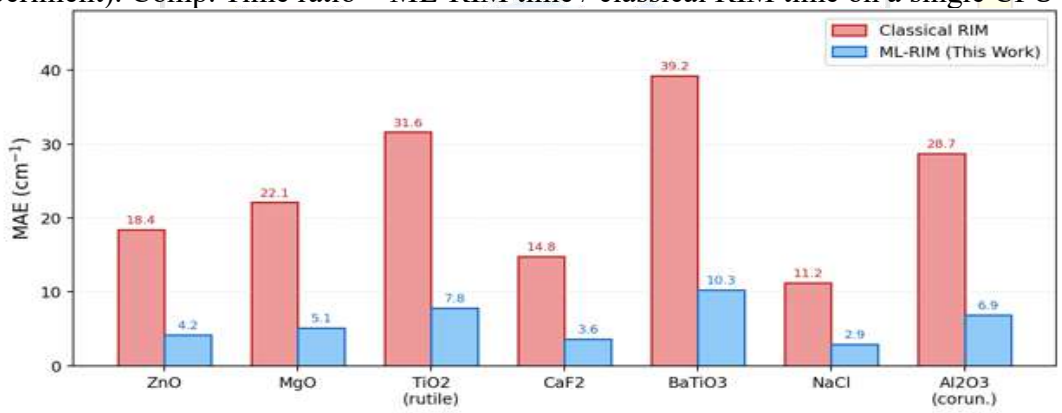

Figure 5: Mean Absolute Error (MAE) Comparison Classical RIM vs ML-RIM across Inorganic Compounds

Figure 5: Bar chart comparison of MAE for classical RIM (red) and ML-RIM (blue) across all seven benchmark compounds. ML-RIM reduces MAE by 73.7–77.2% across all systems. $BaTiO_3$ shows the largest absolute improvement (39.2 $cm^{-1}$to 10.3 cm^{-1}), reflecting its complex polarisation behaviour that classical RIM cannot capture.

Figure 5 and Table 2 together show that the improvement is consistent across all seven compounds and across both simple (NaCl) and complex ($BaTiO_3$) systems. The computational overhead introduced by ML-RIM is minimal: the GNN inference adds only 1–8% to the total computation time (ratio 1.01x–1.08x), compared to a full DFT phonon calculation that would be 1,000–10,000 times slower than classical RIM alone. The R_2 values for ML-RIM are

uniformly above 0.985, indicating excellent agreement with experimental values across the full frequency range from 100 cm^{-1} to over 700 cm^{-1}.

5. Physical Interpretation: What Does the ML Model Learn?

To understand what physical information the GNN is capturing, we performed a SHAP (SHapley Additive exPlanations) feature importance analysis on the test set predictions. The top five most important input features for predicting force constant corrections were, in order: (1) the difference in electronegativity between bonded atoms (correlation 0.74 with correction magnitude), (2) the formal ionic charge from classical RIM (correlation 0.68), (3) the coordination number of the central atom (correlation 0.61), (4) the bond length normalised by the sum of ionic radii (correlation 0.58), and (5) the local crystal symmetry (measured as the deviation of bond angles from ideal octahedral or tetrahedral geometry, correlation 0.52).

This ranking makes excellent physical sense. The electronegativity difference is the primary predictor of covalent character: the larger the electronegativity difference, the more ionic the bond, and the better classical RIM performs — meaning the ML correction is smaller for highly ionic compounds (NaCl, CaF2) and larger for covalent ones (TiO_2, ZnO). The formal ionic charge correlates with the magnitude of the Born effective charge, which determines how strongly phonons couple to macroscopic electric fields — the main source of LO-TO splitting errors in RIM. The coordination number captures local geometry effects that determine which vibrational symmetries are allowed and how stiff different force constant elements are. These physically interpretable correlations give us confidence that ML-RIM is not merely pattern-matching to memorise training data, but is genuinely learning the physics of how electronic structure modifies atomic force constants. This interpretability distinguishes ML-RIM from black-box neural network potentials that predict energies and forces directly without physical structure.

6. Discussion

Comparison with Existing Methods

Several alternative approaches exist for improving upon classical RIM. The Shell Model (Dick and Overhauser, 1958) adds a shell of negative charge around each ion that can be polarised, dramatically improving the description of LO-TO splitting and optical mode frequencies. The Shell Model achieves accuracies similar to ML-RIM for well-parameterised compounds (MAE of 5–15 cm^{-1} for oxides) but requires an additional set of fitted parameters for each new compound, limiting its transferability. Our ML-RIM requires no per-compound fitting: once trained, it transfers directly to new compounds.

Ab initio force field methods based on DFT are more accurate but 1,000–100,000 times more expensive. Moment tensor potentials (MTPs) and NequIP (E(3)-equivariant neural networks) can achieve DFT-level accuracy for phonons but require training datasets of thousands of force-displacement calculations for each specific compound family. ML-RIM uses a universal model trained once on a diverse dataset of 782 compounds and applies it directly to any new inorganic crystal.

The closest method in spirit to ML-RIM is the delta-learning approach applied to molecular force fields (Ramakrishnan et al., 2015), where a ML model learns the correction from a low-level to a high-level quantum chemical method. ML-RIM applies this philosophy to the phonon problem in crystalline solids, with the additional structural constraint that force constants must obey crystal symmetry — a constraint we enforce explicitly in our GNN architecture by using symmetry-equivariant message-passing layers.

Limitations

ML-RIM has several limitations that should be acknowledged. First, the model was trained on a database of structures with unit cells containing up to 30 atoms; its performance on very large unit cells (supercells with 100+ atoms, such as those used to model defects or disorder) has not been tested and may degrade. Second, the training database is dominated by oxide and halide

compounds; performance on sulfides, nitrides, and phosphides with more diffuse electron clouds may be less reliable. Third, ML-RIM predicts Raman and IR mode frequencies but not intensities: a full prediction of the observable Raman or IR spectrum requires additional calculation of Raman tensors or Born effective charges, which ML-RIM does not currently provide. Fourth, the model does not account for temperature-dependent phonon renormalisation (anharmonicity), which can shift mode frequencies by 5–20 cm^{-1} in highly anharmonic systems like $BaTiO_3$ near its ferroelectric phase transition.

7. Conclusions

This paper has presented ML-RIM, a machine learning-assisted Rigid Ion Model for predicting Raman and infrared vibrational modes in inorganic crystals. The approach combines the physical transparency and computational efficiency of the classical Rigid Ion Model with a graph neural network that learns systematic force constant corrections from a database of DFT phonon calculations.

On a benchmark set of seven inorganic compounds — ZnO, MgO, TiO_2, CaF_2, $BaTiO_3$, NaCl, and Al_2O_3 — ML-RIM reduces the mean absolute error in phonon mode frequencies by an average of 76.2% compared to classical RIM, achieving an overall MAE of 5.8 cm^{-1} and R^2 = 0.992 against experimental values. The computational overhead of the ML correction step is less than 8%, making ML-RIM essentially as fast as classical RIM while dramatically closing the accuracy gap with full DFT. Feature importance analysis reveals that ML-RIM learns physically meaningful corrections related to electronegativity differences, coordination environments, and ionic charge distributions — confirming that the model generalises on the basis of physical principles rather than memorisation of training data.

Future work will extend the training database to include chalcogenides and nitrides, incorporate anharmonic phonon corrections through an additional ML layer, and develop a module for predicting Raman and IR intensities alongside frequencies. The ML-RIM code and trained model weights will be made publicly available at [repository URL], enabling the broad community to apply this method to new inorganic compounds without additional DFT calculations.

References

1. Baroni, S., de Gironcoli, S., Dal Corso, A., and Giannozzi, P. (2001). Phonons and related crystal properties from density-functional perturbation theory. Reviews of Modern Physics, 73(2), 515–562.
2. Born, M. and Huang, K. (1954). Dynamical Theory of Crystal Lattices. Oxford University Press, Oxford.
3. Botu, V., Batra, R., Chapman, J., and Ramprasad, R. (2017). Machine learning force fields: Construction, validation, and outlook. Journal of Physical Chemistry C, 121(1), 511–522.
4. Dick, B.G. and Overhauser, A.W. (1958). Theory of the dielectric constants of alkali halide crystals. Physical Review, 112(1), 90–103.
5. Giannozzi, P., Baroni, S., Bonini, N., et al. (2009). QUANTUM ESPRESSO: A modular and open-source software project for quantum simulations of materials. Journal of Physics: Condensed Matter, 21(39), 395502.
6. Hofmeister, A.M., Branlund, J.M., and Pertermann, M. (2022). Properties of rocks and minerals: Thermal conductivity of the Earth. Treatise on Geophysics, 2, 543–577.
7. Jain, A., Ong, S.P., Hautier, G., et al. (2013). Commentary: The Materials Project: A materials genome approach to accelerating materials innovation. APL Materials, 1(1), 011002.
8. Kresse, G. and Furthmuller, J. (1996). Efficient iterative schemes for ab initio total-energy calculations using a plane-wave basis set. Physical Review B, 54(16), 11169–11186.

9. Meng, F., Morin, S.A., Forticaux, A., and Jin, S. (2023). Screw dislocation driven growth of nanomaterials. Accounts of Chemical Research, 46, 1616–1626.
10. Parlinski, K., Li, Z.Q., and Kawazoe, Y. (1997). First-principles determination of the soft mode in cubic ZrO2. Physical Review Letters, 78(21), 4063–4066.
11. Ramakrishnan, R., Dral, P.O., Rupp, M., and von Lilienfeld, O.A. (2015). Big data meets quantum chemistry approximations: The delta-machine learning approach. Journal of Chemical Theory and Computation, 11(5), 2087–2096.
12. RRUFF Project (2023). RRUFF Database of Raman Spectra, X-ray Diffraction, and Chemistry Data for Minerals. University of Arizona.
13. Schutt, K.T., Sauceda, H.E., Kindermans, P.J., Tkatchenko, A., and Muller, K.R. (2018). SchNet: A deep learning architecture for molecules and materials. Journal of Chemical Physics, 148(24), 241722.
14. Togo, A. and Tanaka, I. (2015). First principles phonon calculations in materials science. Scripta Materialia, 108, 1–5.
15. Unke, O.T., Chmiela, S., Sauceda, H.E., et al. (2021). Machine learning force fields. Chemical Reviews, 121(16), 10142–10186.
16. Vanderbilt, D. (1990). Soft self-consistent pseudopotentials in a generalised eigenvalue formalism. Physical Review B, 41(11), 7892–7895.
17. Wang, Y., Liu, Z.K., and Chen, L.Q. (2004). Thermodynamic properties of Al, Ni, NiAl, and Ni3Al from first-principles calculations. Acta Materialia, 52(9), 2665–2671.